Polar alignment states of a ferroelectric nematic liquid crystal on obliquely evaporated SiO<inf>2</inf> surface layers

Liquid Crystals

ISSN: (Print) (Online) Journal homepage: www.tandfonline.com/journals/tlct20

Polar alignment states of a ferroelectric nematic liquid crystal on obliquely evaporated SiO_2 surface layers

Ebba Grönfors & Per Rudquist

To cite this article: Ebba Grönfors & Per Rudquist (03 Mar 2025): Polar alignment states of a ferroelectric nematic liquid crystal on obliquely evaporated SiO_2 surface layers, Liquid Crystals, DOI: 10.1080/02678292.2025.2470124

To link to this article: https://doi.org/10.1080/02678292.2025.2470124

Published online: 03 Mar 2025.

LIQUID CRYSTALS
https://doi.org/10.1080/02678292.2025.2470124

Taylor & Francis
Taylor & Francis Group

Polar alignment states of a ferroelectric nematic liquid crystal on obliquely evaporated SiO_2 surface layers

Ebba Grönfors and Per Rudquist

Department of Microtechnology and Nanoscience, Chalmers University of Technology, Gothenburg, Sweden

ABSTRACT

Spontaneously polar nematic liquid crystals – so-called ferroelectric nematics – add several functionalities to liquid crystal optics and electro-optics, but are also more complex in terms of surface alignment compared to the well-known conventional non-polar nematics. Here we demonstrate that surfaces coated with obliquely evaporated SiO_2 layers facilitate two stable polar surface anchoring states of ferroelectric nematics essentially in the plane of the surface, with azimuthal orientations controlled by the evaporation angle. We also find that the studied material RM734 seems to exhibit a twist, with an estimated pitch of about 10 ± 5 µm in the ferroelectric nematic phase, despite the absence of molecular chirality in RM734. One might speculate whether this twist is intrinsic or a result of the strongly polar ferroelectric nematic relieving costly splay deformations into less costly twist deformations.

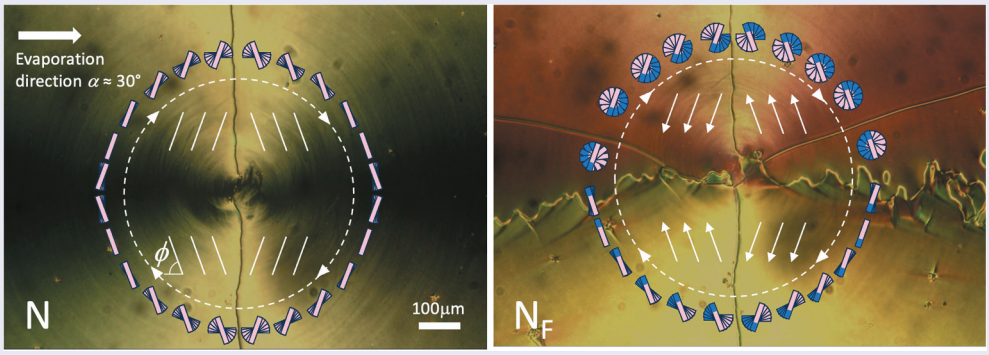

ARTICLE HISTORY
Received 28 November 2024
Accepted 18 February 2025

KEYWORDS
Ferroelectric nematic liquid crystal; surface alignment; oblique evaporation; polar surface anchoring

Introduction

During half a century, commercial LCDs have evolved from simple few-digit displays to 8K TV screens with ~100 million subpixels. During this time, there has been a tremendous materials development in terms of molecular structures and compositions of liquid crystal mixtures to improve display performance, but in fact, the highly sophisticated LCDs of today are based on the same liquid crystal phase as the ones from the 1960s, i.e. the nematic phase (N). This phase – the simplest form of liquid crystal – is a three-dimensional liquid characterised only by long-range orientational order along a unit vector $\mathbf{n}(\mathbf{r})$, called the director, with the special property $\mathbf{n} = -\mathbf{n}$. Hence, the well-known N phase is non-polar, cf Figure 1(a).

In 2017, the first examples of thermotropic nematic-like phases with seemingly spontaneous polar properties were reported in the materials DIO [1] and RM734 [2,3]. Later, Chen et al. reported experimental evidence that the material RM734 in fact exhibited the long sought-after, but until then hypothetic, ferroelectric nematic phase (N_F), having a spontaneous polarisation density $\mathbf{P}$ along the director $\mathbf{n}$ [4], cf Figure 1(b). Ferroelectric nematics is today a hot topic within liquid crystal research [5–16], to large extent motivated also by the fact that the spontaneous polarisation of N_F materials might facilitate new liquid crystal application concepts, not only within optics, electrooptics, and non-linear optics [17], but maybe also for energy harvesting and energy storage devices [18–20].

It was soon observed that the polar nature of N_F materials increases the complexity when it comes to creation of suitable boundary conditions in device-

CONTACT Ebba Grönfors ebba.gronfors@chalmers.se; Per Rudquist per.rudquist@chalmers.se

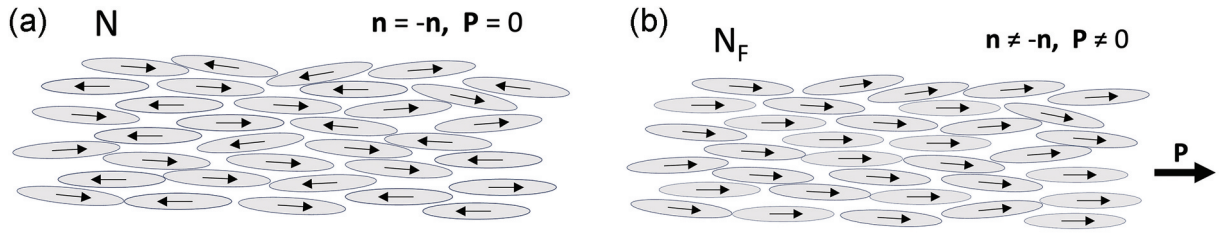

Figure 1. (Colour online) Schematic illustration of (a) the non-polar nematic phase and (b) the polar ferroelectric nematic, built up of molecules with strong axial molecular dipoles. In (a) on average half of the molecules point to the left and half to the right.

type cells. Importantly, Caimi et al. observed that conventional, rubbed polyimide (PI) layers, that impose planar homogeneous in-plane anchoring of N materials, impose polar in-plane anchoring of the N_F phase [21]. Consequently, in sample cells with antiparallel rubbing at the two PI surfaces, twisted director fields are formed, to match the two polar boundary conditions to the inherent polarity of the ferroelectric nematic cf Figure 2. In any types of future N_F application, it will likely be crucial to have control of both alignment and polarity direction at the bounding surfaces.

Moreover, there are a few reports suggesting that the N_F phase of RM734 also has an intrinsic tendency to twist normal to the director, with equal probability for left- and right-handed twist [22]. Such spontaneous reflection symmetry breaking was in fact already proposed by Khachaturyan, for a hypothetical polar nematic phase [23].

In this study we explore inorganic surface layers of obliquely evaporated SiO_2 as alignment layers for the archetype N_F material RM734. We find that on such SiO_2 surfaces there are two stable polar director states, symmetrically oriented at the angle $\pm\phi$ about the evaporation plane, where ϕ depends on the evaporation angle α. For moderate evaporation angles $\alpha \approx 30°(45°)$, $\phi \approx \pm 70°(80°)$, i.e. the surface director makes a large angle from the evaporation plane. At large evaporation angles, $\alpha \approx 80°$, the two surface states are situated closer to the evaporation plane, at $\phi \approx \pm 35°$. Moreover, ϕ is found to decrease with decreasing temperature even though quantitative results are difficult to obtain, as will be discussed. Importantly, we find that in the N_F

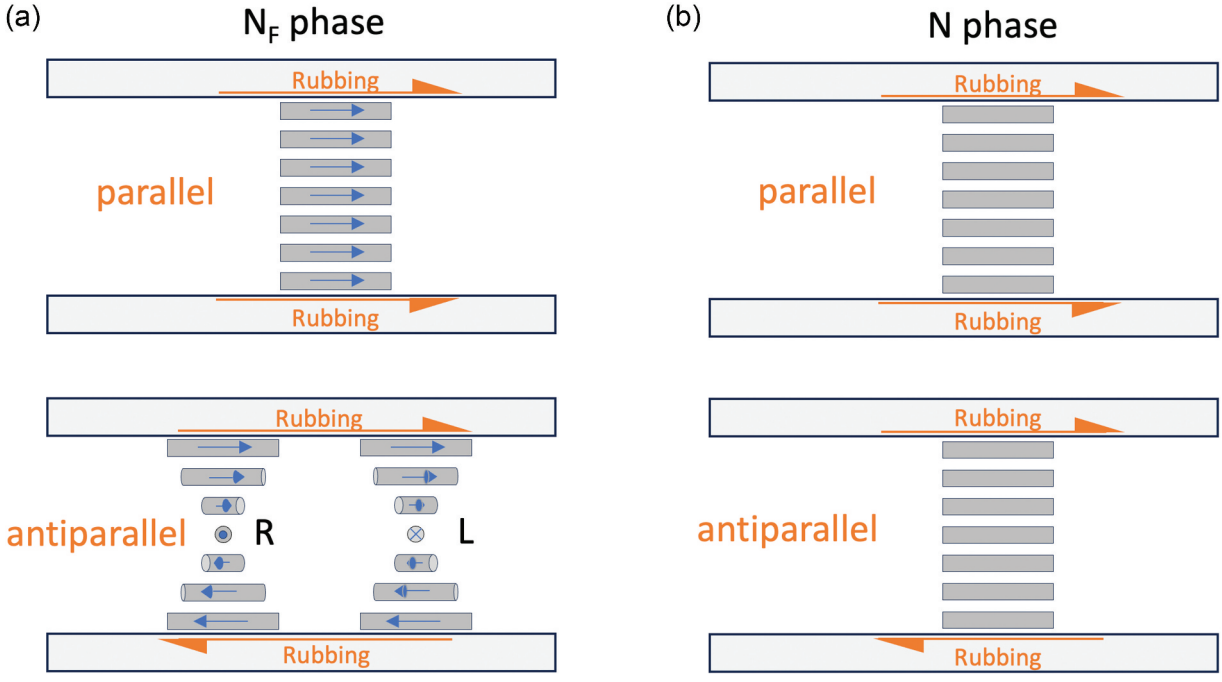

Figure 2. (Colour online) Alignment of the N_F and N phases in sample cells with linearly rubbed polyimide surface layers. (a) In the N_F phase, parallel rubbing conditions provide a non-twisted planar state, while antiparallel rubbing conditions gives ± 180° twisted states due to the polar in-plane alignment on rubbed surfaces. (b) In the non-polar N phase, both parallel and antiparallel rubbing give homogeneous states.

phase there seems to be an intrinsic twist normal to the polarisation direction, with the same probability for both signs of twist. The spontaneous breaking of mirror symmetry in the N_F phase of RM734 conforms well with the recent findings reported by Kumari et al. [22].

Inorganic surface alignment layers

Alignment of nematic liquid crystals by means of obliquely evaporated inorganic surface layers was first demonstrated by Janning [24] and later studied further by several groups [25–27]. Generally, for small evaporation angles $\alpha \leq 30°$, i.e. when the evaporation direction is rather close to the substrate normal, the director was found to orient normal to the evaporation plane ($\phi = 90°$), and hence, parallel to the surface, cf. Figure 3(c). For shallow incidence of the evaporation beam, i.e. for $\alpha \geq 80°$, the director instead turned out to align parallel to the evaporation plane, with a pretilt of several degrees [24], cf Figure 3(a). This picture was further modified when it was found that in a range of intermediate evaporation angles two symmetric alignment directions at $\pm\phi(\alpha)$ were found, symmetrically positioned about the evaporation plane [28–31], cf Figure 3(b). For example, Jägemalm et al. showed that the azimuthal angle $\phi(\alpha)$ varies 'continuously' from 90° to 0° in the interval $66° < \alpha < 76°$ for the standard nematic mixture E7 on obliquely evaporated SiO_x surfaces [29]. Moreover, they found that ϕ depends on temperature, with a continuous change from $\phi = 90°$ at $T = 55°C$, to $\phi = 10°$ at $T = 25°C$ at an evaporation angle of $\alpha = 74°$. In addition to this azimuthal change of the surface alignment the director pretilt simultaneously increased from 0° to about 20°.

We can now speculate what would happen when a ferroelectric nematic liquid crystal is used in the three cases of Figure 3. Let us first consider the two limiting cases of small and large values of α. From symmetry we see that if the N_F director ends up normal to the evaporation plane (cf. Figure 3(c)), the surface alignment direction on SiO_2 should be non-polar, i.e. **P** would point in either of two opposite directions with the same probability. In such polar domains the director could in fact also adopt a finite pretilt. On the other hand, if the alignment direction is parallel to the evaporation plane (Figure 3(a)) the alignment is always polar, as the (pretilted) states with opposite sign of **P** in the evaporation plane would be non-degenerate. Finally, the intermediate cases $\pm\phi$ in Figure 3(b) should also be polar by symmetry. Hence, for intermediate evaporation angles, we could expect a two-fold, degenerate polar alignment of the N_F phase, and this also turns out to be the case.

Experimental

The liquid crystal RM734 (iso – 188°C – *N* – ~130°C – N_F), cf. Figure 4, was kindly synthesised and supplied by E. Korblova and D. M. Walba at University of Colorado at Boulder. Very recently, Thoen et al. by means of high resolution calorimetry reported the existence of a narrow additional N_X phase between N and N_F [32]. Another batch of RM734 from Instec Inc. was acquired through University of Stuttgart, Germany. The nematic mixture E7 (iso – 56°C – N) was purchased from Synthon Chemicals.

The sample cells were made from 75 mm × 75 mm ITO-coated glass plates. The plates were cleaned in a megasonic bath of deionised water:ammonia

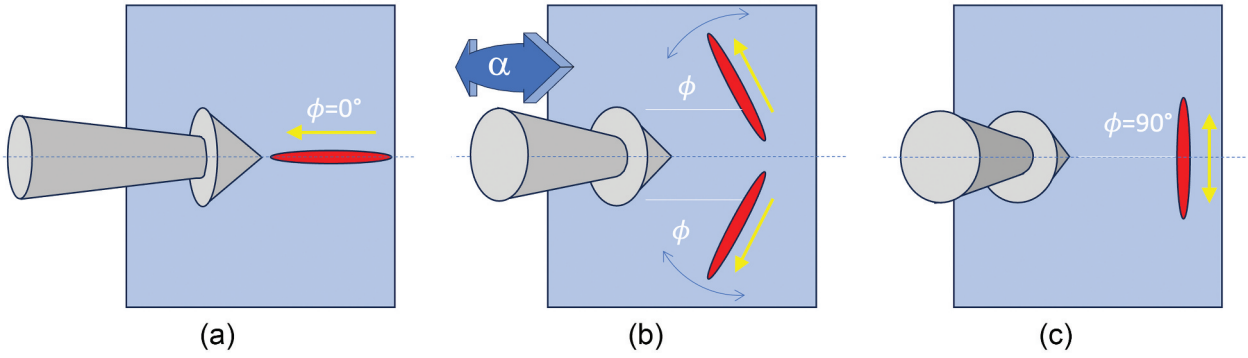

Figure 3. (Colour online) Schematic illustration of alignment (red) of nematic LCs on obliquely evaporated inorganic surface layers [24,29]. At grazing incidence of the evaporation beam (a) the director becomes parallel to the evaporation plane ($\phi = 0°$) with a slight pretilt. For small evaporation angles (c) the director becomes normal to the evaporation plane ($\phi = 90°$). For intermediate angles (b), the director may adopt two degenerate alignment orientations at $\pm\phi$ (α). In the case of ferroelectric nematics, the anchoring in c) is non-polar by symmetry, while the anchorings in a) and b) are polar, as indicated with yellow arrows. Evaporation beam direction indicated schematically as grey arrow.

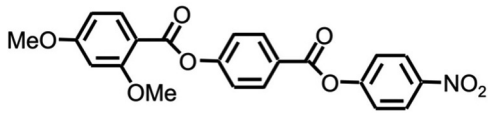

Figure 4. Molecular structure of RM734.

(concentration 25%):hydrogen peroxide (concentration 30%) in relations 6:1.2:1.2, for four 10 minute cycles, and rinsed and dried in a rinser dryer under a nitrogen atmosphere after each cycle.

SiO_2 alignment layers were deposited using an AVAC HVC600 evaporator, with electron beam heating of the SiO_2 target, at an evaporation rate of 1 Å/s, at a pressure of about 2×10^{-6} mbar, to a nominal film thickness of 200 Å, as deposited on the oscillating quartz crystal thickness sensor. The distance from the target to the substrate was about 400 mm. The relatively large size of the substrate (75 mm x 75 mm) makes the evaporation angle α vary about ± 5° between the edges of the substrate being nearest and farthest away from the SiO_2 target, cf Figure 5(a). The tilt of the substrate, and hence the adjustment of the evaporation angle could be made with an accuracy of ± 5°. For the experiments with rubbed PI alignment layers, we used PI2610 (DuPont), diluted to 0.5% concentration in dimethylsulfoxide (DMSO), spin-coated onto the cleaned substrates at 5000 rpm for 30 s, prebaked at 100°C for 60 s, and subsequently cured in an oven at 300°C for 3 h. Linear rubbing of PI layers were carried out using a commercial substrate rubbing machine (LCTec Automation).

For a major part of the study, we used a new type of hybrid cell, combining an obliquely evaporated SiO_2 coated plate with a circularly rubbed PI-coated plate, see Figure 5(b). This **E**vaporated/**C**ircularly **R**ubbed **C**ell (ECRC) is a variant of the **C**ircularly **R**ubbed **C**ell (CRC) geometry used by Rudquist as a method for identification of the ferroelectric nematic phase [33]. For circular rubbing of the PI layer, we used an electric pillar drilling machine, equipped with a flat chuck of about 8 mm diameter coated with a piece of commercial rubbing cloth. While keeping the PI coated substrate fixed on the drilling machine table, the rotating chuck was gently pushed towards the surface for about a second. On each 75 mm x 75 mm substrate 25 (5 × 5 in a square matrix) circular rubbing zones were created. One circularly rubbed PI coated substrate and one SiO_2 coated substrate were then assembled and glued together using UV-curing glue (Norland Adhesive 68), using a home-built programmable glue dispenser and a commercial substrate aligning machine (Ciposa). Silica spheres of diameter 4 µm were dispersed in the glue, securing a cell gap in the range of 3.8–4 µm depending on the pressure during substrate assembly. After curing of the glue under UV light each assembly was cut into 25 sample cells. The evaporation plane in individual cells from each assembly cuts the opposite CRC surface at slightly

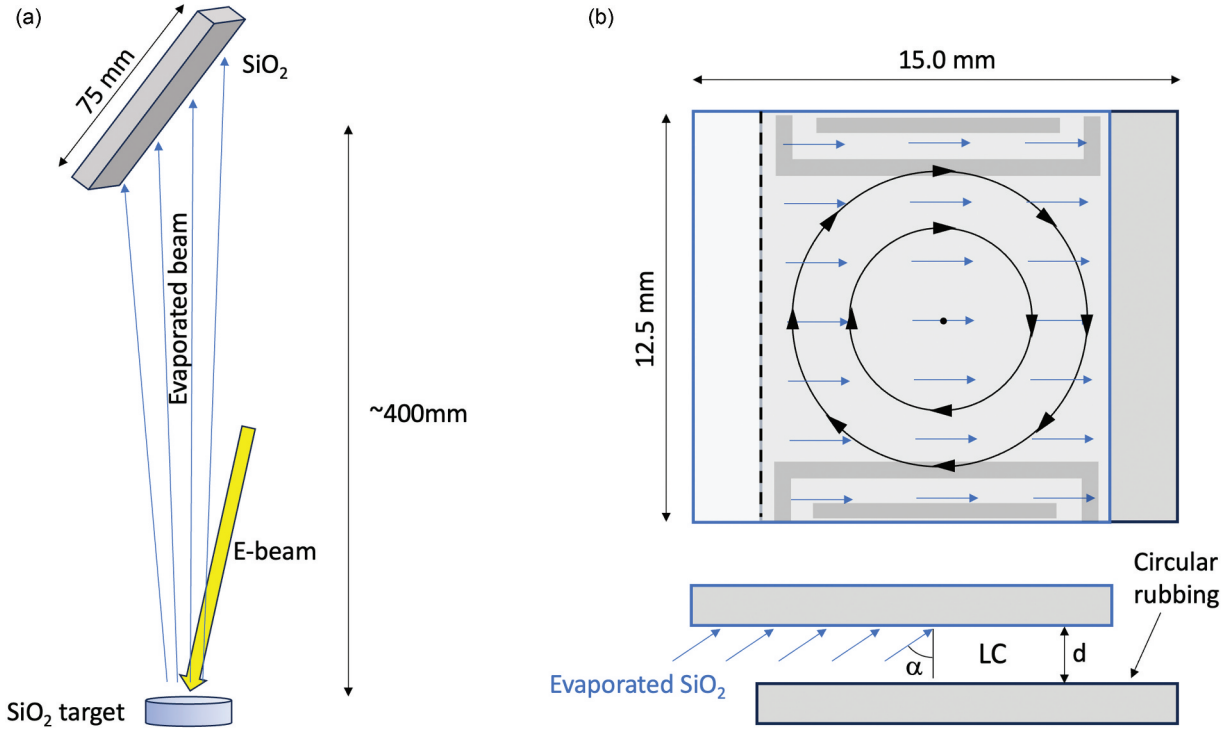

Figure 5. (Colour online) (a) Schematics of the evaporation setup. (b) schematics of the ECRC. The circular rubbing direction (lower surface) is indicated in black and the evaporation direction (top surface) in blue arrows. The cell gap d ≈ 4 µm.

different orientations, depending on the position of the cell on the large assembly. But this does not matter for the investigation, thanks to the circular symmetry of the CRC surface; the orientation of the evaporation plane in each cell can be determined from the symmetry of the imposed liquid crystal defect structure in each cell, as all diameters on the circularly rubbed surface are equivalent.

ECRCs were used to probe the alignment at the SiO_2 surface as follows: The twist of the nematic liquid crystal director varies with the azimuthal angle about the centre of circular rubbing. ECRC regions in which there is no twist, i.e. where the local mutual alignment directions on the two surfaces are parallel, can be brought into extinction by rotating the microscope turntable so that the director field in these regions are parallel to any of the crossed polarisers. As we know the local rubbing direction on the circularly rubbed surface, we then also know the director orientation ϕ on the opposing SiO_2 surface.

Two additional sets of sample cells were fabricated with two SiO_2 coated surfaces, where the evaporation directions were parallel and anti-parallel respectively. Care was taken of choosing the proper cells from each assembly, to minimise effects of misalignment of the mutual evaporation planes over the surfaces of the large substrates.

The sample cells were filled with liquid crystal by means of capillary forces in the isotropic phase (at $T \approx$ 190°C, in the case of RM734). The optical studies were made with polarised optical microscopy (POM), and a temperature controlled warm-stage fixed onto the microscope turntable.

Results and discussion

Nematic E7 in ECRCs

To verify the ECRC-method for measuring ϕ, sample cells were filled with the standard, non-polar commercial nematic material E7, with three different nominal evaporation angles of the SiO_2, $\alpha \approx 30°$, $\alpha \approx 45°$, and $\alpha \approx 80°$, respectively. The alignment direction ϕ on the SiO_2 surface was found from the azimuthal extinction positions of the cell between crossed polarisers. In POM we could see that all three cells exhibited two disclination lines along the diameter at 12 and 6 o'clock (clock face notation). Just below the nematic to isotropic phase transition two extinction positions were observed normal to the disclination lines when the disclination line was orientated along one of the polarisers. Hence, at high temperatures the director was found to be normal to the evaporation plane ($\phi \approx 90°$) for all three evaporation angles. For $\alpha \approx 30°$ and for $\alpha \approx 45°$, we observed essentially no temperature dependence of ϕ, i.e. $\phi\ (\alpha \approx 30°) \approx \phi\ (\alpha \approx 45°) \approx 90°$ for all temperatures below the clearing point. For $\alpha \approx 80°$, however, a clear temperature dependence was observed. On cooling through the nematic phase, the director at the SiO_2 surface stayed normal to the evaporation plane ($\phi \approx 90°$) in the interval $56°C > T > 44°C$, but thereafter it decreased continuously to about $\phi \approx 65°$ at room temperature. This change in ϕ with temperature is qualitatively similar to what was observed by Jägemalm et al [29], for SiO_x mediated alignment of E7 with $\alpha \approx 70°$. Although two sets of domains with $\pm\phi$ were observed in some ECRCs containing E7, one of the two surface orientations tended to dominate across each cell. We might speculate that this could be an effect of the increased surface director pretilt at larger α. As mentioned above, Jägemalm et al. showed that the pretilt at large α could be as high as 20° for E7 on SiO_x [29]. In combination with the circular rubbing on the opposite surface, this would lead to varying amounts of splay deformation across the cell. This in turn, in order to minimise the total elastic energy, could in principle make one sign of ϕ more favourable than the other. Notably, the two disclination lines stayed azimuthally fixed even when ϕ changed, indicating that the defect lines are pinned to one of the surfaces of the cell rather than suspended in the bulk.

Nematic and ferroelectric nematic RM734 in ECRC

A similar set of ECRCs were then filled with RM734. A main difference compared to E7 was that $\phi \neq 90°$, also for the smaller evaporation angles $\alpha \approx 30°$, and $\alpha \approx 45°$. In the nematic phase (Figure 6(a)) we generally found two disclination lines as in E7 at 12 and at 6 o'clock and two sharp, jagged, domain boundaries, along the two radii at 9 and 3 o'clock, separating domains with different optical properties. By rotation of the cell between crossed polarisers we could observe two sets of extinction arms, revealing four azimuthal positions with non-twisted director fields. The configuration in Figure 6(a) is consistent with the director at the SiO_2 surface making a discontinuous jump between $-\phi$ and $+\phi$ at the jagged domain boundaries, as well as at the disclination lines at 12 and 6 o'clock, as schematically indicated. We draw the conclusion that there are two possible surface states, $\pm\phi$, for the director at the SiO_2 surface, just as for E7. Furthermore, from the positions of the flips in surface orientation, we suggest that the material as a rule locally chooses the one of the two possible surface states that produces a minimum twist between the SiO_2 coated surface and the circularly rubbed PI surface. Importantly, the overall north–south symmetry in the optical properties in the photograph of Figure 6(a) shows that the north and the south halves are each

other's mirror images. Similar principal textures were found for α ≈ 45°, although somewhat less clear-cut. At α ≈ 80°, the difference was even larger, with no clear domain boundaries appearing at 9 and 3 o'clock. Instead, ϕ tended to keep the same sign across larger domains, reminiscing of the E7 cells with the same high value of α.

The temperature dependence of the orientation of the surface states on the SiO_2 surface was determined as described above. While the cells with α ≈ 30° and α ≈ 45° exhibited little or no temperature dependence of the surface director orientation, the α ≈ 80° cell displayed a significant change in ϕ with temperature, cf Figure 7. When slowly decreasing the temperature, at about 1°C/min, and waiting several minutes at each temperature before measuring ϕ, we observed a continuously decreasing ϕ from ~80° at 180°C to ~60 at 135°C, cf Figure 7(a). On the other hand, after rapid virgin cooling (~10°/min) from the isotropic to the measurement temperature, a much larger temperature dependence in ϕ was observed, cf Figure 7(b). Now the final value of ϕ varied from ~70° at 180°C to ~13° at 135°C, and when cycled these values appeared to stay fixed in each cell based on their respective first cooling. Note that in Figure 7(b), each individual datapoint is taken from individual ECRCs, after capillary filling in the isotropic phase, and after subsequent virgin cooling down to the measurement temperature. Figure 7(c) depicts ϕ (T) during slow cooling (~1°/min) measured during the first cooling and on cooling in the same sample after being heated and cooled several times. It is evident from Figure 7 that the measured value of ±ϕ depends on the history of the sample. A slight dependence of ϕ on the history of the sample was also mentioned by Jägemalm et al. for the nematic E7 on SiO_x surfaces [29].

At the transition from N to the ferroelectric N_F phase there is a dramatic change in the texture, cf Figure 6(b). In the polar phase there are now two disclinations where the twist changes handedness and four boundaries on the SiO_2 surface where ϕ switches sign. Moreover, the different optical properties (different colour) in the north and south halves show that the amount of twist differs between the north and south halves. This can only be explained by the surface states at the SiO_2 surface being *in-plane polar*. We already know that the rubbed PI surface (circular rubbing) gives in-plane polar surface alignment in the N_F phase. The cell with α ≈ 30° shown in Figure 6 represents the most clear-cut evidence of polar two-fold alignment states in the N_F state.

Intrinsic twist of the N_F phase

It is relatively straight forward to determine the surface director orientation ±ϕ in the N phase, by means of ECRCs. There were always well-defined twist-free regions that gave extinction of light for certain azimuthal positions of the turntable between crossed polarisers. In the N_F phase, however, we could only occasionally find such twist-free regions that revealed the director orientation on the SiO_2 surface. Especially for α ≈ 80°, there were no azimuthal orientations of the ECRC between crossed polarisers that gave extinction of light. Hence, for α ≈ 80° the N_F phase wants to be *twisted for all combinations of alignment directions at the opposing surfaces*. This can be explained by letting

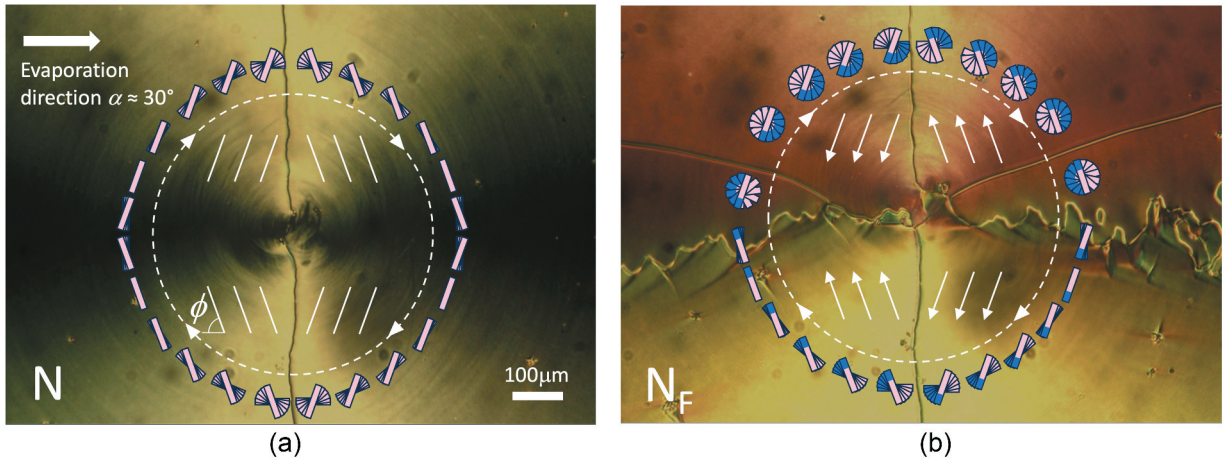

Figure 6. (Colour online) 4 µm thick ERC cell filled with RM734; circular rubbing on the lower (—) and SiO_2 (α ≈ 30°) on the upper substrate. The surface alignment on the SiO_2 surface is indicated with solid lines (N (a)) and arrows (N_F (b)), respectively. The up-down asymmetry in the N_F case (b) reveals the polar nature of the two surface states on the SiO_2 surface.

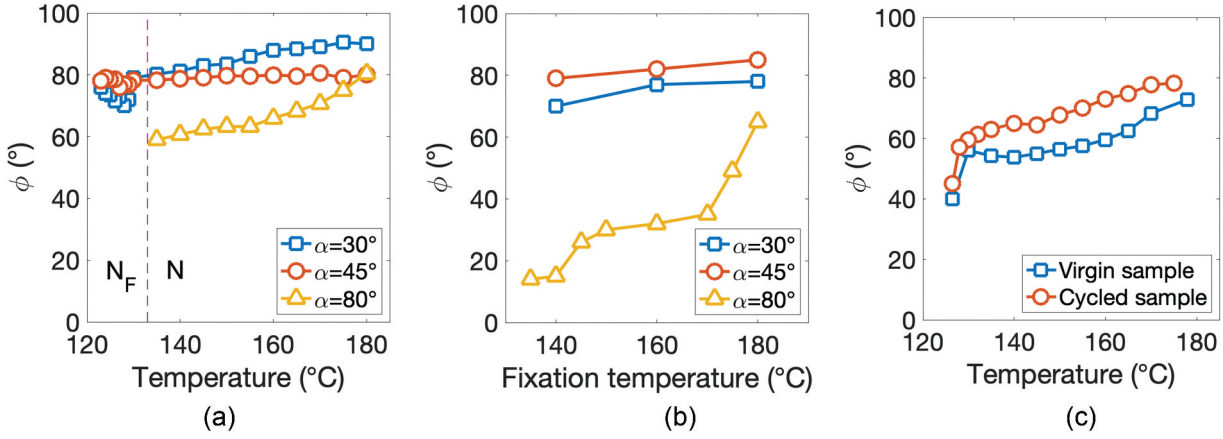

Figure 7. (Colour online) Surface director angle ϕ from the evaporation plane as function of temperature for different evaporation angles α. (a) slow cooling, (b) rapid virgin cooling from isotropic, individual sample cells for each point, and (c) difference between first (virgin) cooling and repeated cooling after heating. Generally, ϕ increases with decreasing temperature. It is evident that ϕ depends on the history of the sample. Below $T = 130$°C (in the ferroelectric nematic phase) only a few points could be measured, cf. Table 1, as helix free domains are unstable, due to the inherent twist of the N_F phase. Lines in graphs are a guide to the eye.

Table 1. Estimated values of ϕ in the N_F phase, measured from metastable helix-free domains in ECRCs.

Evaporation angle α	Alignment angle ±ϕ
~30°	~70°
~45°	~80°
~80°	~35°

the lowest energy state of the N_F phase be helical (right or left-handed with equal probability). This would constitute a spontaneous breaking of mirror symmetry at the N-N_F transition, where the ground state of the N_F phase in RM734 is twisted, like a chiral nematic, with the two twist senses being degenerate. This would be in agreement with the results from Kumari [22]. For example, if the intrinsic pitch in the N_F phase would be 8 µm, the director would like to make a 180° twist between the surfaces in a cell gap of 4 µm. Hence, the twist elastic energy in the material will be minimised in the regions where the alignment directions in the ECRC are antiparallel, and it will have its maximum where the alignment directions are parallel, e.g. 0° (untwisted) or 360° twisted. This would be at the diametrically opposite position in the cell, in the case where ϕ is constant across the whole SiO_2 surface. But, importantly, the sign of ϕ usually changes between alternating domains. This means that even in the case where the natural twist would be less than 180°, there is no guarantee to find extinction anywhere, as the adopted alignment directions may not be parallel anywhere.

A twist, intrinsic or induced, also may affect ϕ due to the twist elastic torque, locally or globally, forcing **n** at the surfaces to deviate from the easy axis in favour of getting closer to the desired amount of twist. With an intrinsic twist, this means that the measured values of ϕ would be affected in the cases where parallel easy axes exist somewhere in the cell, as the position of the untwisted state might be shifted. Previous studies have observed a similar effect on rubbed surfaces, where **n** in the N_F phase deviates from the easy axis to avoid twisting too much [34,35], and it would be reasonable to assume the same could apply to avoid twisting too little. For sake of simplicity, we assume that the deviation between ϕ and the easy axis in a cell gap about 4 µm is small.

Let us now look at Figure 6(b) in detail. There are several sectors in the cell, separated by disclination lines or domain boundaries. Four of these boundaries are located on the SiO_2 surface and reveal where ϕ changes sign. These domain boundaries are set in the N phase. We see that these do not tend to move but are pinned to set positions once they have appeared. Thus, we cannot draw any certain conclusions about ϕ in the N_F phase based on the exact position of these domain boundaries. The two disclinations at 10 and 2 o'clock are pure disclinations located in the bulk of the material, and there is a jump between right/left and left/right 180° twist. This allows us to determine ϕ in the cases where this set of disclinations appear, as they appear where the alignment directions are antiparallel.

Below the jagged domain boundaries, the twist needed to satisfy both boundary conditions is near either 0° or 360°. For many cells, such as the one shown in Figure 6, the optical properties of the south domains are similar to what is observed in the N phase,

indicating that in this specific case a twist near 0° is more favourable than one near 360°.

Finally, two sample cells were studied where both surfaces had the SiO_2 surface treatment with $\alpha = 30°$, with parallel and anti-parallel evaporation directions respectively. When filled with RM734, the two cells appeared identical between crossed polarisers in both N and N_F, indicating that when $\phi \approx 90°$ the boundary conditions are in principle non-polar. Figure 8 shows one of the cells being cycled between N and N_F. When entering the N_F phase, the material is at first untwisted, but then relaxes to a ~ 180° twisted state. This indicates that a 180° twist requires a lower energy in the material than both 0° and 360°. From this, we can deduce that the optimal twist for a cell gap just below 4 µm must be somewhere between 90° and 270°, corresponding to an intrinsic pitch of roughly 10 ± 5 µm.

In 1974 Khachaturyan proposed that an achiral nematic with a spontaneous polarisation should be unstable to twist [23], i.e. in the absence of external actions, the bulk director spontaneously would form a helix (left-, or right-handed with the same probability) normal to the local polarisation (cholesteric structure) to minimise the total energy. At this stage, we can only say that there might be a helical structure in the ferroelectric nematic RM734. An intrinsic helical structure has been observed by Kumari et al, in samples with one linearly rubbed cell surface and one cell surface with tangentially degenerate planar surface anchoring [22]. They found that the pitch depends on the cell geometry, where a cell gap of 3 µm corresponds to a pitch of 6.5 ± 0.1 µm. Our estimation of the pitch being 10 ± 5 µm for a cell gap just below 4 µm appears to be in good agreement with the observations of Kumari et al. But in this discussion, we have not considered any effects of possible high pretilt at the SiO_2 surface, which could at least in principle induce a twist to supress costly splay. The large value of the splay elastic constant, relative to those for twist and bend, would originate from divergence induced polarisation charge density, $\rho = -\nabla \cdot \mathbf{P}$. This was recently discussed by Kumari et al. in relation to conic sections in ferroelectric nematics [36].

Circularly rubbed cells with both surfaces covered with rubbed PI, where all mutual alignment directions are present, could constitute an alternative method for estimating the intrinsic pitch in ferroelectric nematics in addition to their ability to distinguish between polar (one disclination) and non-polar (two disclinations) materials. One should then use CRCs with a cell gap << the N_F pitch for simple calibration and analysis.

We suggest that obliquely evaporated surface layers might facilitate bistable operation of future N_F electro-optic devices, where the optic axis of the N_F could be

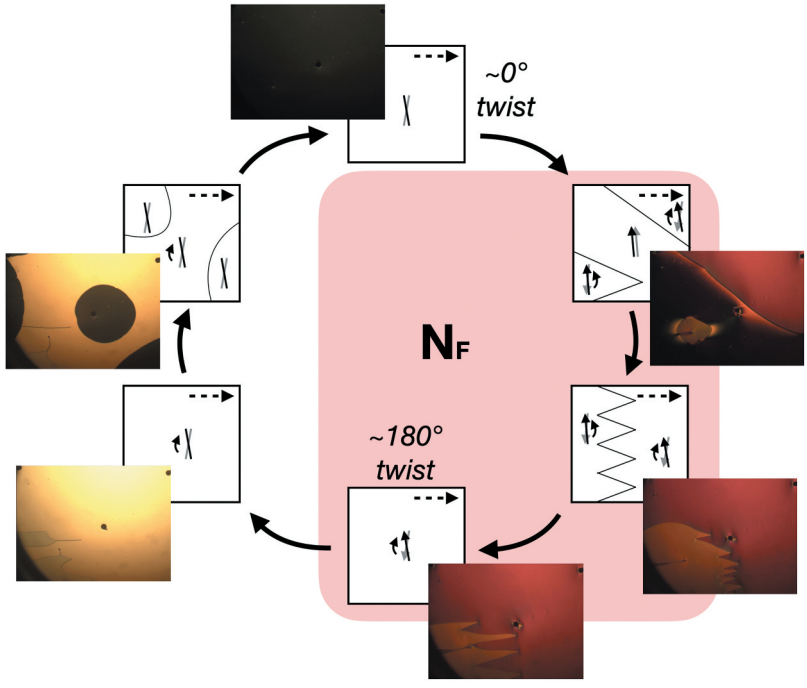

Figure 8. (Colour online) RM734 in a cell with both surfaces treated with SiO_2 with $\alpha \approx 30°$, viewed between crossed polarisers and cycled between N and N_F. When the material enters the N_F phase, it is approximately untwisted at first, but then relaxes first into left- and right-handed domains with ~ 180° twist, followed by one of them dominating the other due to being marginally closer to the optimal twist. Upon returning to the N phase, the ~ 180° twist eventually relaxes back into an approximately untwisted state.

switched between ±ϕ in the plane of the device, by means of in-plane electric pulses of opposite polarity. For uniform polar states, the helix-free structure might need to be surface-stabilised, reminiscent of a surface-stabilised ferroelectric device [37]. But, with multistable surface states from obliquely evaporated inorganic surface layers, also possible intrinsically twisted states might be utilised. This, at least in principle, opens for devices with bistable, tristable, or even quadrustable configurations combining surface-stabilised, and twist-stabilised, stable and metastable states.

Conclusions

We have studied the surface alignment of the archetype ferroelectric nematic material RM734 on obliquely evaporated surface layers. We find a two-fold degenerate alignment, analogous to what is found for conventional nematics, with the two states ±ϕ symmetrically positioned about the evaporation plane. The surface orientation angle ϕ was determined by means of ECRCs, combining an obliquely evaporated surface layer on one surface with a linearly rubbed surface on the other. From the domain and twist configurations, we could also show that the two-fold surface alignment states are in-plane polar.

Furthermore, our results indicate the possibility of an intrinsic twist in the ferroelectric nematic phase of RM734, as reported earlier in the literature [22]. We estimated that this pitch is about 10 ± 5 µm.

Acknowledgments

The first batch of RM734 was kindly synthesised and supplied by E. Korblova and D. M. Walba at University of Colorado at Boulder. Another batch of RM734 from Instec Inc. was acquired through University of Stuttgart, Germany. The sample cells were made in the Myfab Nanofabrication Laboratory at Chalmers

Disclosure statement

No potential conflict of interest was reported by the author(s).

Funding

This work was supported by the Swedish Research Council (Vetenskapsrådet) under Grant [2023–04853].

References

[1] Nishikawa H, Shiroshita K, Higuchi H, et al. A fluid liquid-crystal material with highly polar order. Adv Mater. 2017;29(43):1702354. doi: 10.1002/adma.201702354

[2] Mandle RJ, Cowling SJ, Goodby JW. A nematic to nematic transformation exhibited by a rod-like liquid crystal. Phys Chem Chem Phys. 2017;19(18):11429–11435. doi: 10.1039/C7CP00456G

[3] Mandle RJ, Cowling SJ, Goodby JW. Rational design of rod–like liquid crystals exhibiting two nematic phases. Chemistry. 2017;23(58):14554–14562. doi: 10.1002/chem.201702742

[4] Chen X, Korblova E, Dong D, et al. First-principles experimental demonstration of ferroelectricity in a thermotropic nematic liquid crystal: polar domains and striking electro-optics. PNAS. 2020;117(25):14021–14031. doi: 10.1073/pnas.2002290117

[5] Mertelj A, Cmok L, Sebastián N, et al. Splay nematic phase. Phys Rev. 2018;10(8):41025. doi: 10.1103/PhysRevX.8.041025

[6] Sebastián N, Cmok L, Mandle RJ, et al. Ferroelectric-ferroelastic phase transition in a nematic liquid crystal. Phys Rev Lett. 2020;124(3):37801. doi: 10.1103/PhysRevLett.124.037801

[7] Chen X, Zhu Z, Magrini MJ, et al. Ideal mixing of paraelectric and ferroelectric nematic phases in liquid crystals of distinct molecular species. Liquid Cryst. 2022;49(11):1531–1544. doi: 10.1080/02678292.2022.2058101

[8] Brown S, Cruickshank E, Storey JMD, et al. Multiple polar and non-polar nematic Phases. Chemphyschem. 2021;22(24):2506–2510. doi: 10.1002/cphc.202100644

[9] Chen X, Korblova E, Glaser MA, et al. Polar in-plane surface orientation of a ferroelectric nematic liquid crystal: polar monodomains and twisted state electro-optics. PNAS. 2021;118(22):e2104092118. doi: 10.1073/pnas.2104092118

[10] Madhusudana NV. Simple molecular model for ferroelectric nematic liquid crystals exhibited by small rod-like mesogens. Phys Rev E. 2021;104(1):14704. doi: 10.1103/PhysRevE.104.014704

[11] Mandle RJ, Sebastián N, Martinez-Perdiguero, et al. On the molecular origins of the ferroelectric splay nematic phase. Nat Commun. 2021;12(1):4962. doi: 10.1038/s41467-021-25231-0

[12] Mandle RJ. A new order of liquids: polar order in nematic liquid crystals. Soft Matter. 2022;18(27):5014–5020. doi: 10.1039/d2sm00543c

[13] Cruickshank E, Rybak P, Majewska MM, et al. To Be or not to Be polar: the Ferroelectric and antiferroelectric nematic phases. ACS Omega. 2023;8(39):36562–36568. doi: 10.1021/acsomega.3c05884

[14] Chen X, Martinez V, Korblova E, et al. Antiferroelectric smectic ordering as a prelude to the ferroelectric nematic: introducing the smectic Z_A phase. In: Proceedings of the 18th International Conference on Ferroelectric Liquid Crystals - Polarity and Chirality in Soft Matter; 2021 sept 6–10; Ljubljana, Slovenia. arXiv preprint, 2021. arXiv:2112.14222.

[15] Chen X, Martinez V, Korblova E, et al. The smectic Z_A phase: antiferroelectric smectic order as a prelude to the ferroelectric nematic. PNAS. 2023;120(8):e2217150120. doi: 10.1073/pnas.2217150120

[16] Nacke P, Manabe A, Klasen-Memmer M, et al. New examples of ferroelectric nematic materials showing evidence for the antiferroelectric smectic-Z phase. Sci Rep. 2024;14(1):4473. doi: 10.1038/s41598-024-54832-0
[17] Folcia CL, Ortega J, Vidal R, et al. The ferroelectric nematic phase: an optimum liquid crystal candidate for nonlinear optics. Liquid Cryst. 2022;49(6):899–906. doi: 10.1080/02678292.2022.2056927
[18] Máthé MT, Himel MSH, Adaka A, et al. Liquid piezoelectric materials: linear electromechanical effect in fluid ferroelectric nematic liquid crystals. Adv Funct Mater. 2024;34(18):2314158. doi: 10.1002/adfm.202314158
[19] Rupnik PM, Cmok L, Sebastián N, et al. Viscous mechano-electric response of ferroelectric nematic liquid. Adv Funct Mater. 2024;34(38):2402554. doi: 10.1002/adfm.202402554
[20] Hassan F, Yang D, Saadoui L, et al. Bulk photovoltaic effect in ferroelectric nematic liquid crystals. Opt Lett. 2024;49(16):4662–4665. doi: 10.1364/OL.527568
[21] Caimi F, Nava G, Barboza R, et al. Surface alignment of ferroelectric nematic liquid crystals. Soft Matter. 2021;17(35):8130–8139. doi: 10.1039/D1SM00734C
[22] Kumari P, Basnet B, Lavrentovich MO, et al. Chiral ground states of ferroelectric liquid crystals. Science. 2024;383(6689):1364–1368. doi: 10.1126/science.adl0834
[23] Khachaturyan AG. Development of helical cholesteric structure in a nematic liquid crystal due to the dipole-dipole interaction. J Phys Chem Solids. 1975;36(10):1055–1061. doi: 10.1016/0022-3697(75)90044-X
[24] Janning JL. Thin film surface orientation for liquid crystals. Appl Phys Lett. 1972;21(4):173–174. doi: 10.1063/1.1654331
[25] Guyon E, Pieranski P, Boix M. On different boundary conditions of nematic films deposited on obliquely evaporated plates. Lett Appl Eng Sci. 1973;1:19.
[26] Monkade M, Boix M, Durand G. Order electricity and oblique nematic orientation on rough solid surfaces. Europhys Lett. 1988;5(8):697. doi: 10.1209/0295-5075/5/8/006
[27] Barberi R, Giocondo M, Sayko GV. Planar nematic anchoring on SiO-coated substrates. Il Nuovo Cimento D. 1994;16(7):895–900. doi: 10.1007/BF02456740
[28] Jerome B, Pieranski P. Wetting and multistable anchorings in nematics. J Phys Fr. 1988;49(9):1601–1613. doi: 10.1051/jphys:019880049090160100
[29] Jägemalm P, Komitov L. Temperature induced anchoring transition in nematic liquid crystals with two-fold degenerate alignment. Liquid Cryst. 1997;23(1):1–8. doi: 10.1080/026782997208604
[30] Barbero G, Jägemalm P, Zvezdin AK. Temperature-induced surface transition in nematic liquid crystals oriented by evaporated SiOx. Phys Rev E Stat Nonlin Soft Matter Phys. 2001;64(2 Pt 1):021703. doi: 10.1103/PhysRevE.64.021703
[31] Barberi R, Giocondo M, Iovane M, et al. Nematic anchoring transitions on bistable SiO films driven by temperature and impurities. Liquid Cryst. 1998;25(1):23–29. doi: 10.1080/026782998206461
[32] Thoen J, Cordoyiannis G, Korblova E, et al. Calorimetric evidence for the existence of an intermediate phase between the ferroelectric nematic phase and the nematic phase in the liquid crystal RM734. Phys Rev E. 2024;110(1):014703. doi: 10.1103/PhysRevE.110.014703
[33] Rudquist P. Revealing the polar nature of a ferroelectric nematic by means of circular alignment. Sci Rep. 2021;11(1):24411. doi: 10.1038/s41598-021-04028-7
[34] Abe S, Shibata Y, Kimura M, et al. Self-consistent explanation of the untwist alignment of ferroelectric nematic liquid crystals with decreasing cell thickness and deviation of the surface easy axis experimented upon using the brewster angle reflection method. Crystals. 2024;14(2):157. doi: 10.3390/cryst14020157
[35] Kamifuji H, Nakajima K, Tsukamoto Y, et al. Effect of rubbing symmetry on polarization distribution in ferroelectric nematic liquid crystal cells. Appl Phys Express. 2023;16(7):071003. doi: 10.35848/1882-0786/acde40
[36] Kumari P, Kurochkin O, Nazarenko VG, et al. Conic sections in ferroelectric nematics: experiments and mathematical modeling. Phys Rev Res. 2024;6(4):043207. doi: 10.1103/PhysRevResearch.6.043207
[37] Clark NA, Lagerwall ST. Submicrosecond bistable electro-optic switching in liquid crystals. Appl Phys Lett. 1980;36(11):899–901. doi: 10.1063/1.91359